A Computational Perspective on Mechanism and Kinetics of the Reactions of CF3C(O)OCH2CF3 with OH radicals and Cl atoms at 298 K

ARTICLE *in* JOURNAL OF FLUORINE CHEMISTRY · APRIL 2014

Impact Factor: 1.95 · DOI: 10.1016/j.jfluchem.2014.01.017

4 AUTHORS:

Dr. Nand Kishor Gour
Tezpur University
12 PUBLICATIONS **39** CITATIONS
SEE PROFILE

Ramesh Chandra
Indian Institute of Technology Roorkee
186 PUBLICATIONS **1,539** CITATIONS
SEE PROFILE

Hari Singh
Deen Dayal Upadhyaya Gorakhpur University
51 PUBLICATIONS **404** CITATIONS
SEE PROFILE

Bhupesh Kumar Mishra
D. N. Government College, Itanagar, Arunac…
45 PUBLICATIONS **279** CITATIONS
SEE PROFILE

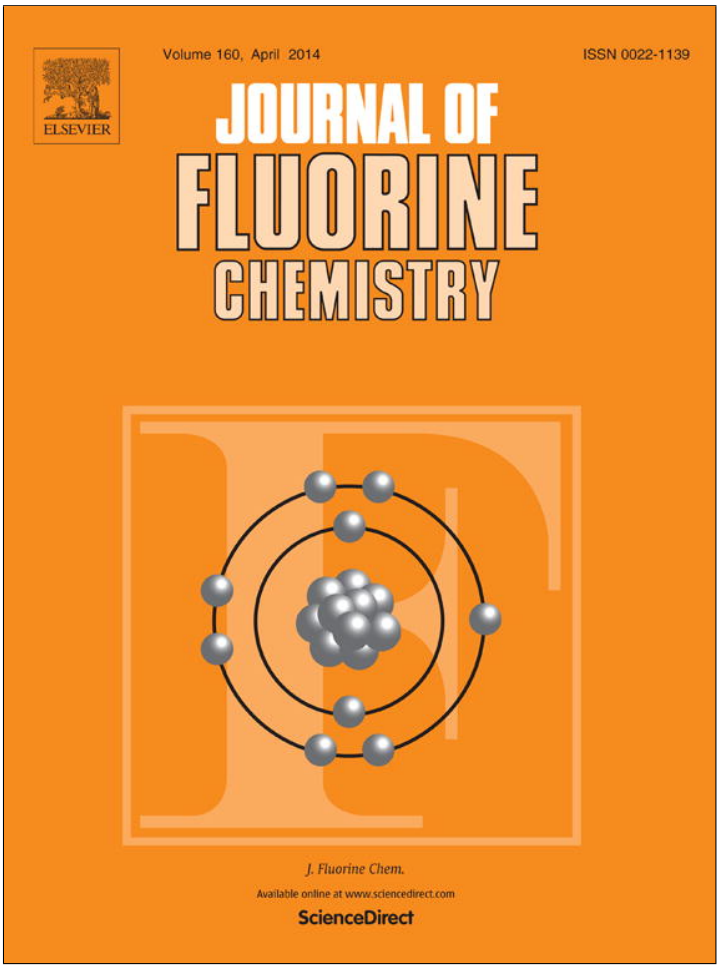

Journal of Fluorine Chemistry 160 (2014) 64–71

Contents lists available at ScienceDirect

Journal of Fluorine Chemistry

journal homepage: www.elsevier.com/locate/fluor

A computational perspective on mechanism and kinetics of the reactions of $CF_3C(O)OCH_2CF_3$ with OH radicals and Cl atoms at 298 K

Nand Kishor Gour [a], Ramesh Chandra Deka [b], Hari Ji Singh [a], Bhupesh Kumar Mishra [b,*]

[a] Department of Chemistry, D.D.U. Gorakhpur University, Gorakhpur, Uttar Pradesh 273009, India
[b] Department of Chemical Sciences, Tezpur University, Napaam, Tezpur, Assam 784 028, India

ARTICLE INFO

Article history:
Received 7 December 2013
Received in revised form 2 January 2014
Accepted 23 January 2014
Available online 2 February 2014

Keywords:
H-abstraction
Fluoroesters
Potential energy surface
Canonical transition state theory
Boltzmann distribution

ABSTRACT

Theoretical investigations are carried out on the gas-phase reactions of $CF_3C(O)OCH_2CF_3$, 2,2,2-trifluoroethyl trifluoroacetate (TFETFA) with OH radicals and Cl atoms by means of modern DFT methods. Two conformers relatively close in energy have been identified for TFETFA, both of them are likely to be important in the temperature range of our study. Reaction profiles are modeled including the formation of two pre-reactive and post-reactive complexes. The optimized geometries, frequencies and minimum energy path are obtained at hybrid density functional model, M06-2X level using 6-31+G(d,p) basis set. The single point energy calculation was further refined by using 6-311++G(d,p) and Aug-cc-pVTZ basis sets. The existence of transition states on the corresponding potential energy surface is ascertained by performing intrinsic reaction coordinate (IRC) calculation. Theoretically calculated rate constants at 298 K and using the canonical transition state theory (CTST) are found to be in good agreement with the experimentally measured ones. Using group-balanced isodesmic reactions, the standard enthalpies of formation for $CF_3C(O)OCH_2CF_3$ and radical generated by hydrogen abstraction, $CF_3C(O)OCHCF_3$, are also reported for the first time. The estimated atmospheric lifetime of TFETFA is expected to be 0.15 years.

1. Introduction

Recently, volatile organic compound especially hydrofluoroethers (HFEs) is designed and widely recommended as a third generation replacement for chlorofluorocarbons (CFCs), Hydrofluorocarbon (HFCs) and hydrochlorofluorocarbon (HCFCs) in applications such as cleaning of electronic equipments, heat transfer fluid in refrigerators, lubricant deposition and foam blowing agents [1–3]. Considerable attention has been paid in recent years to perform experimental and theoretical studies on the decomposition kinetics of HFEs [4–12] to determine the impact of these compounds on atmospheric pollution and global warming. The major degradation pathways of HFEs in the atmosphere may be initiated by photolytic degradation with OH radicals and Cl atoms in coastal areas and also possibly with chloride containing aerosol of highly industrialized urban areas. It is well established that the fluorinated esters (FESs) are the primary products of the atmospheric oxidation of HFEs [13–16]. For example, $CF_3C(O)OCH_2CF_3$, 2,2,2-trifluoroethyl trifluoroacetate (TFETFA) can be produced from the OH radicals and Cl atoms initiated oxidation of $CF_3CH_2OCH_2CF_3$ (HFE-356mf-f) in the atmosphere [17]. Like HFEs, FESs also undergoes photochemical oxidation in troposphere with atmospheric oxidants, OH radicals or Cl atoms. The degradation of FESs produce environmentally burdened product like trifluoroacetic acid (TFA), CO_2, and COF_2. TFA detected in surface waters has no known sink apart from rainwater and this species may impact on agricultural and aquatic systems [18]. Thus, it is important to study the kinetics and mechanistic degradation pathways of FESs for complete assessment of atmospheric chemistry as well as explore the impact of FESs on environment. Recently, Bravo et al. [13] have used density functional theory and the methodology developed by their group to predict infrared spectra and calculate radiative efficiencies (REs) and global warming potentials (GWPs) for a number of FESs. Lestard et al. [19] have been determined the molecular structure of two conformers of TFETFA in the gas-phase by electron-diffraction supplemented by ab initio (MP2) and DFT calculations using 6-311++G(d,p) basis set.

In our present work, we have studied the mechanism and kinetics of H-abstraction reaction between TFETFA with OH radicals (reaction (R1)) and Cl atoms (reaction (R2)) using DFT methods.

$$CF_3C(O)OCH_2CF_3 + OH \rightarrow CF_3C(O)OCHCF_3 + H_2O \quad (R1)$$

$$CF_3C(O)OCH_2CF_3 + Cl \rightarrow CF_3C(O)OCHCF_3 + HCl \quad (R2)$$

* Corresponding author. Tel.: +91 3712267008.
E-mail address: bhupesh@tezu.ernet.in (B.K. Mishra).

0022-1139/$ – see front matter © 2014 Elsevier B.V. All rights reserved.
http://dx.doi.org/10.1016/j.jfluchem.2014.01.017

Blanco et al. [20] studied the kinetics of hydrogen abstraction reactions with Cl atoms for TFETFA by the relative kinetic method at 298 K and atmospheric pressure (760 Torr). The experimental rate constant was reported as $k(Cl + CF_3C(O)OCH_2CF_3) = (1.18 \pm 0.43) \times 10^{-15}$ cm^3 molecule^{-1} s^{-1}. In other reports, Blanco and Teruel [21] studied the kinetics of the reactions of OH radicals with selected fluoroacetates by the relative kinetic method at 296 ± 2 K and atmospheric pressure (760 ± 10 Torr) and reported a rate constant value of $k(OH + CF_3C(O)OCH_2CF_3) = (1.05 \pm 0.23) \times 10^{-13}$ cm^3 molecule^{-1} s^{-1}. In earlier report Stein et al. [22] experimentally investigated the thermal decomposition of haloalkoxy radical $CF_3C(O)OCH(O)CF_3$ produced by OH and Cl-initiated oxidation of TFETFA in a FTIR smog chamber. Three loss processes were identified at 296 K which include reaction with O_2 to form $CF_3C(O)OC(O)CF_3$, α-ester rearrangement to produce CF_3CO and harmful $CF_3C(O)OH$ (TFA) and thermal decomposition. Among the three reaction pathways, reaction with O_2 is the dominant pathway but at the same time contribution of α-ester rearrangement and thermal decomposition cannot be ignored. In another report, Blanco et al. [23] studied the product distribution of TFETFA with Cl atoms using a 1080 L quartz-glass reaction chamber at (296 ± 2) K and concluded that reaction of O_2 is the major reaction pathways. Interestingly in their report it was also mentioned that α-ester rearrangement pathways is negligible and no TFA was observed. However, to the best of our knowledge no theoretical study has been made on this reaction to understand its mechanism and thermochemistry. In addition, the knowledge of accurate enthalpy of formation ($\Delta_f H^{\circ}_{298}$) for $CF_3C(O)OCH_2CF_3$ and $CF_3C(O)OCHCF_3$ radical generated from $CF_3C(O)OCH_2CF_3$ is of vital importance for determining the thermodynamic properties and the modeling of atmospheric process. However, no theoretical or experimental study on standard enthalpy of formation has been reported so far for these species. Here, we predict the enthalpies of formation using isodesmic reactions by performing single-point energy calculation at high level of theory, G2(MP2) with geometrical parameters obtained at the MPWB1K/6-31+G(d,p) level.

2. Results and discussion

Geometry optimization of TFETFA molecule predicts two possible conformers (SC1 and SC2) and their structures are shown in Fig. 1. The conformer of lowest energy (SC1) found here is also identical with that reported by Lestard et al. [19]. Since these two conformers are close in energy (0.65 kcal mol^{-1}), both of them (SC1 and SC2) need to be considered while studying the reactions (R1) and (R2). The two conformers differ mainly in the orientation of C3–H2 bond relative to the C–O–C–C backbone. The C4–C3–O2–C2 dihedral angle is 179.98 in the SC1 conformer; whereas the same is 99.93 in the SC2 conformer. The calculated enthalpy of reactions ($\Delta_r H^{\circ}$) at 298 K for the reaction of TFETFA with OH radicals and Cl atoms are recorded in Table 1. The reaction enthalpy ($\Delta_r H^{\circ}$) values for reactions (R1) and (R2) are −14.71 and −3.57 kcal mol^{-1}, respectively which clearly shows that both reactions are exothermic in nature thus thermodynamic facile. Two reactant complexes (RCs) and product complexes (PCs) are validated at the entrances and exits of the two H-abstraction channels by OH radicals, which means that this abstraction channels may proceed via indirect mechanism. The optimized structures of the pre-reaction (RC) and post-reaction (PC) complexes are shown in Fig. 1. As shown in the reaction energy profile diagram in Fig. 2, two reaction complexes ($RC1_{SC1}$ and $RC2_{SC2}$) were located at the entry point of reaction channels (R1) from two conformers of $CF_3C(O)OCH_2CF_3$. On other hand, two product complexes ($PC1_{SC1}$ and $PC2_{SC2}$) were found at the exit channels of the reaction (R1). The reaction complexes are formed due to interaction between $CF_3C(O)OCH_2CF_3$ and OH radicals through C–H···O and OH···F/O hydrogen bonding, whereas the two product complexes are resulted from the hydrogen bonding interaction between $CF_3C(O)OCHCF_3$ radical and H_2O molecule.

As can be seen from the geometrical parameters and stereographical orientation, the hydrogen atoms in the $-CH_2$ group are equivalent in SC1 and SC2 conformers. We could locate two transition states ($TS1_{SC1}$ and $TS1_{SC2}$) each for hydrogen abstraction by OH radicals from the SC1 and SC2 conformers of TFETFA. Meanwhile, for hydrogen abstraction by Cl atoms, the same transition state was found from both conformers of TFETFA. Therefore, we have presented only one transition state ($TS2_{SC1}$) from the most stable conformer SC1. The structural parameters obtained at M06-2X/6-31+G(d,p) level for reactants SC1, SC2, OH and Cl, reaction complexes (RCs), transition states ($TS1_{SC1}$, $TS2_{SC1}$ and $TS1_{SC2}$), product complexes (PCs) and products ($CF_3C(O)OCHCF_3$, H_2O and HCl) involved in reactions (R1) and (R2) are given in Fig. 1. These species are also optimized at MPWB1K/6-31+G(d,p) level of theory and corresponding results are shown in the same figure for comparison. As shown in Fig. 1 the optimized geometrical parameters obtained at two levels of theory are reasonably in good agreement with each other. Moreover, Fig. 1 reveals that the geometrical parameters obtained at M06-2X/6-31+G(d,p) level of theory are in very good agreement with the reported values by Lestard et al. [19] at MP2 and DFT levels. Thus, structural parameters obtained from M06-2X/6-31+G(d,p) were used for all energetics and kinetic calculations. Transition states search was made along the minimum energy path on a relaxed potential energy surface. In the process of hydrogen abstraction reaction from a C–H bond, the C–H bond breaks and a new O–H bond is formed giving rise to the water molecule. Thus, during the formation of transition states, the important structural parameters have to be observed are one of the C–H bond of the leaving hydrogen and the newly formed bond between H and O atoms in the OH radical. Visualization of the optimized structure of $TS1_{SC1}$ further reveals the elongation of C–H (C3–H2) bond length from 1.085 to 1.243 Å (almost an 14% increase) at MPWB1K and 1.092–1.221 Å at the M06-2X level (almost 12%) whereas the newly formed H–O (O3–H2) bond is increased from 0.953 to 1.236 Å resulting in an increase of about 30% at MPWB1K while at M06-2X level this increment is about 32%. Similarly, the structure of $TS1_{SC2}$ reveals that the breaking C–H bond (C3–H2) is found to be longer by 13% at MPWB1K and 10% at M06-2X than the observed C–H bond length in isolated $CF_3C(O)OCH_2CF_3$; whereas the forming O···H bond length is longer by 32–37% than the O–H bond length in H_2O. The fact that the elongation of forming bond is found to be larger than that of the breaking bond indicates that the barrier of the reaction (R1) is near the corresponding reactants. This means the reaction (R1) will proceed via early transition state structure. For the transition state structure of the hydrogen abstraction initiated by Cl atoms ($TS2_{SC1}$), the length of the breaking C–H (C3–H2) bond increases from 1.085 to 1.388 Å (28% increase) at MPWB1K and 1.092–1.405 Å at the M06-2X level whereas the newly formed H–Cl bond is increased from 1.272 to 1.447 Å at MPWB1K (about 13%) and 1.280 to 1.449 Å (almost an 28% increase) at M06-2X level. It indicates that the barrier of this reaction (R2) lies near the product and the reaction with Cl atoms will proceed via a late transition state. Results obtained during frequency calculations for species involved in reactions (R1) and (R2) are recorded in Table 2. These results show that the reactants and products have stable minima on their potential energy surface characterized by the occurrence of only real positive vibrational frequencies. Transition states (TS) are characterized by the occurrence of only one imaginary frequency at 1665i, 913i and 1572i cm^{-1} for $TS1_{SC1}$, $TS2_{SC1}$ and $TS1_{SC2}$, respectively at M06-2X level while these values amount to be 1744i, 1166i and 1452i cm^{-1} for $TS1_{SC1}$, $TS2_{SC1}$ and $TS1_{SC2}$, respectively at MPWB1K level of

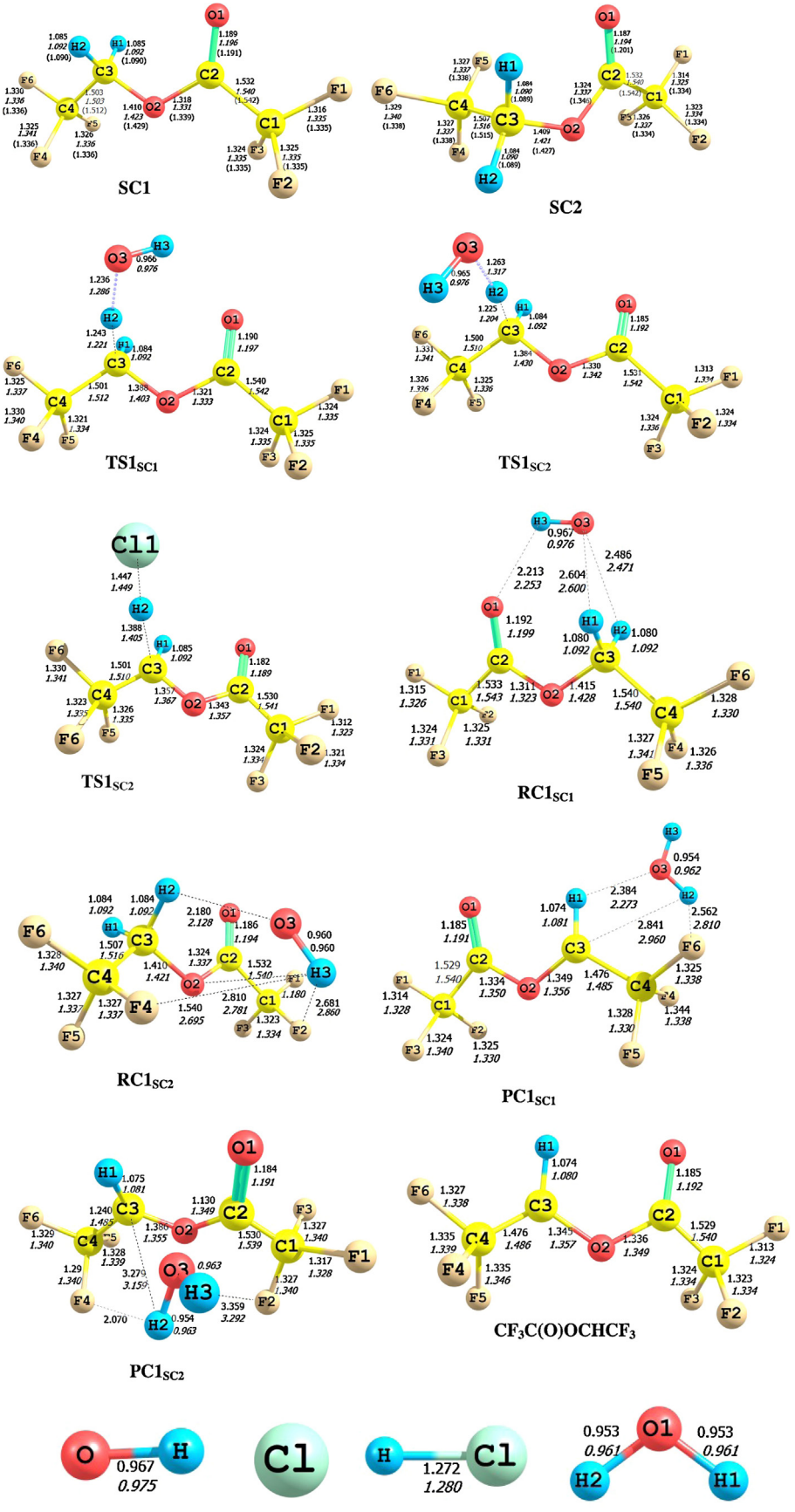

Fig. 1. Optimized geometries of species at MPWB1K level and M06-2X (italic values) levels of theory. The values given in parentheses are taken from Ref. [19]. Bond lengths are in angstroms.

Table 1
Reaction enthalpies at M06-2X/6-31+G(d,p) and barrier heights obtained at various level of theories. All values are in kcal mol^{-1}.

Conformer	Reaction channel	$\Delta_r H^\circ$	TS	ΔE_0		
				M06-2X/ 6-31+G(d,p)	M06-2X/ 6-311++G(d,p)	M06-2X/ Aug-cc-pVTZ
SC1	R1	−14.55	TS_{1SC1}	2.17	2.32	2.66
	R2	−3.41	TS_{2SC1}	4.15	3.88	3.96
SC2	R1	−15.20	TS_{1SC2}	3.24	3.27	3.50
	R2	−4.06	$TS2_{SC2}$	4.15	3.88	3.96
	Average R1 [a]	−14.71				
	Average R2 [a]	−3.57				

[a] Weighted average as per Boltzmann distribution law as given in Eq. (5).

theory. Visualization of the vibration corresponding to the calculated imaginary frequencies shows a well defined transition state geometry connecting reactants and products during transition. The existence of transition state on the potential energy surface is further ascertained by intrinsic reaction coordinate (IRC) calculation performed at the same level of theory using the Gonzalez–Schlegel steepest descent path in the mass-weighted Cartesian coordinates with a step size of 0.01(amu$^{1/2}$ – bohr) [24]. The IRC plots for transition states clearly authenticate a smooth transition from reactants to products on the potential energy surface.

The associated energy barriers corresponding to the reactions (R1) and (R2) at different level of theories are also recorded in Table 1. These results show that energy barriers for H atom abstraction reaction of $CF_3C(O)OCH_2CF_3$ with OH radical are 2.17 and 3.24 kcal mol^{-1} for conformers SC1 and SC2 at M06-2X/6-31+G(d,p) level of theory. Also for the H atom abstraction reaction of $CF_3COOCH_2CF_3$ with Cl atoms, the barrier heights are found to be 4.15 kcal mol^{-1} at M06-2X/6-31G+(d,p) level of theory. Literature survey reveals that there is no experimental data available for the comparison of the energy barrier for the H-atom abstraction reaction of TFETFA by OH radicals and Cl atoms. A potential energy diagram of the title reactions is constructed with the results obtained at M06-2X/6-31+G(d,p) level of theory and is shown in Fig. 2. These energies are plotted with respect to the ground state energy of reactants ($CF_3C(O)OCH_2CF_3$+OH/Cl) arbitrarily taken as zero.

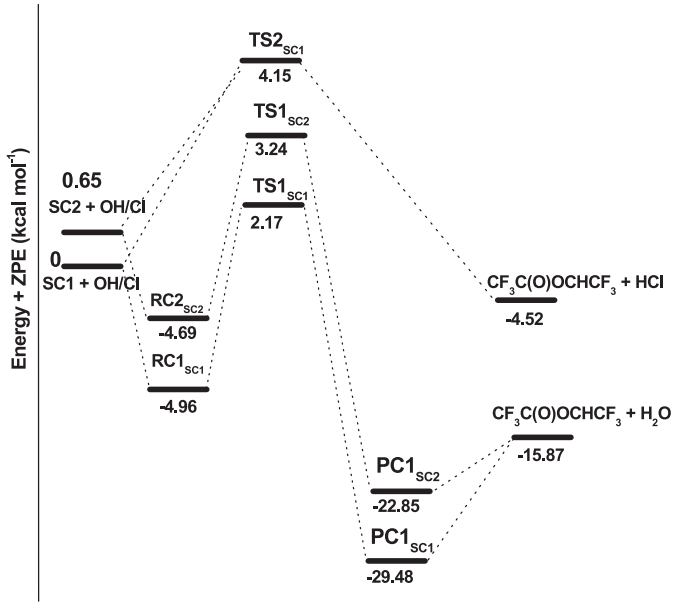

Fig. 2. Schematic potential energy profile for hydrogen abstraction reactions of $CF_3C(O)OCH_2CF_3$ with OH radicals and Cl atoms. Relative energies (in kcal mol^{-1}) of different species are calculated at M06-2X/6-31+G(d,p) level of theory.

The standard enthalpy of formation ($\Delta_f H^\circ_{298}$) at 298 K for $CF_3C(O)OCH_2CF_3$ and the radical generated from hydrogen abstraction ($CF_3C(O)OCHCF_3$) can be valuable information for understanding the mechanism and thermochemical properties of their reactions and most importantly for atmospheric modeling, but these values are not yet reported. The group-balanced isodesmic reactions, in which the number and types of bonds are conserved, are used as working chemical reactions herein to calculate the $\Delta_f H^\circ_{298}$ for $CF_3C(O)OCH_2CF_3$ and radical generated from hydrogen abstraction reactions. Here, following isodesmic reactions are used to estimate the enthalpies of formation of these species:

a. For $CF_3C(O)OCH_2CF_3$

$$CF_3C(O)OCH_2CF_3 + CH_4 \rightarrow CF_3CF_3 + CH_3C(O)OCH_3 \quad (R3)$$

$$CF_3C(O)OCH_2CF_3 + CH_4 + CH_3CH_3 \rightarrow CH_3COCH_3 + CH_3OCH_3 + CF_3CF_3 \quad (R4)$$

$$CF_3C(O)OCH_2CF_3 + CH_3CH_3 \rightarrow CH_3C(O)OCH_2CH_3 + CF_3CF_3 \quad (R5)$$

b. For $CF_3C(O)OCHCF_3$

$$CF_3C(O)OCHCF_3 + CH_4 \rightarrow CF_3C(O)OCH_2CF_3 + CH_3 \quad (R6)$$

$$CF_3C(O)OCHCF_3 + CH_3Cl \rightarrow CF_3C(O)OCH_3 + CF_3CHCl \quad (R7)$$

$$CF_3C(O)OCHCF_3 + CH_4 + CHFCl_2 \rightarrow CH_3C(O)OCH_3 + CF_3CF_3 + CFCl_2 \quad (R8)$$

All geometrical parameters of the species involved in the isodesmic reactions (R3)–(R8) were optimized at the MPWB1K and M06-2X levels using 6-31+G(d,p) basis set. The energies of these species optimized at MPWB1K level were then refined at the G2(MP2) level of theory. At first we have calculated the reaction enthalpies ($\Delta_r H^\circ_{298}$) of the Isodesmic reactions (R3)–(R8) as mentioned above using total energies of the species obtained at different levels including thermal correction to enthalpy estimated at MPWB1K/6-31+G(d,p) level. Since, the $\Delta_r H^\circ_{298}$ value corresponds to the difference of the enthalpy of formation ($\Delta_f H^\circ_{298}$) values between the products and the reactants, the $\Delta_f H^\circ_{298}$ values of the reactant and product species can be easily evaluated by combining them with the known enthalpies of formation of the reference compounds involved in our Isodesmic reaction schemes. The experimental $\Delta_f H^\circ_{298}$ values for CH_4: −17.91 kcal mol^{-1}, CH_3OCH_3: −44.0 kcal mol^{-1}, CH_3CH_3: −20.01 kcal mol^{-1} and CH_3: 34.85 kcal mol^{-1} are taken from Ref. [25], CH_3Cl: −19.76 kcal mol^{-1} $CHFCl_2$: −67.72 kcal mol^{-1} and $CFCl_2$: −22.32 kcal mol^{-1} are taken from Ref. [26], CF_3CF_3: −321.20 kcal mol^{-1} [27], CF_3CHCl: −131.93 kcal mol^{-1} [28],

Table 2
Harmonic vibrational frequencies of reactants, transition states and products at M06-2X/6-31+G(d,p) and MPWB1K/6-31+G(d,p) (italic values in parentheses) level of theories.

Species	Vibrational frequencies (cm^{-1})
SC1	32, 47, 54, 84, 146, 202, 245, 281, 327, 364, 409, 456, 526, 537, 556, 605, 655, 752, 791, 860, 940, 982, 1092, 1219, 1223, 1243, 1257, 1312, 1326, 1343, 1431, 1480, 1499, 1926, 3126, 3191 *(20, 31, 47, 82, 147, 199, 245, 284, 332, 363, 417, 461, 533, 542, 562, 615, 666, 765, 809, 875, 955, 998, 1113, 1238, 1249, 1263, 1279, 1335, 1346, 1364, 1466, 1503, 1525, 1958, 3176, 3244)*
SC2	30, 43, 49, 55, 177, 207, 266, 295, 336, 390, 417, 470, 526, 531, 554, 599, 678, 745, 789, 855, 874, 1010, 1081, 1197, 1247, 1254, 1257, 1312, 1331, 1356, 1423, 1459, 1489, 1937, 3139, 3212 *(16, 45, 55, 117, 173, 206, 267, 295, 339, 398, 426, 476, 532, 539, 561, 608, 691, 759, 808, 872, 889, 1027, 1101, 1221, 1267, 1276, 1280, 1334, 1353, 1383, 1457, 1490, 1515, 1968, 3192, 3269)*
OH	3758 *(3868)*
$RC1_{SC1}$	20, 34, 47, 56, 68, 83, 121, 160, 204, 229, 258, 281, 301, 332, 374, 417, 458, 526, 539, 607, 658, 753, 792, 862, 939, 983, 1081, 1215, 1230, 1254, 1262, 1313, 1324, 1441, 1481, 1498, 1910, 3130, 3194, 3777 *(12, 23, 36, 47, 69, 82, 93, 154, 194, 203, 251, 268, 287, 337, 377, 424, 463, 533, 545, 563, 616, 669, 765, 809, 878, 950, 1008, 1101, 1239, 1257, 1271, 1281, 1336, 1350, 1370, 1475, 1507, 1522, 1945, 3181, 3252, 3874)*
$RC1_{SC2}$	35, 54, 65, 81, 99, 104, 168, 186, 209, 250, 262, 273, 331, 367, 398, 422, 459, 525, 537, 558, 607, 658, 753, 788, 859, 934, 991, 1107, 1216, 1229, 1249, 1253, 1311, 1330, 1347, 1437, 1481, 1502, 1944, 3125, 3192, 3754 *(55, 81, 86, 94, 117, 146, 168, 208, 219, 253, 303, 333, 344, 389, 401, 413, 459, 529, 542, 556, 607, 658, 751, 804, 848, 931, 1006, 1074, 1202, 1223, 1227, 1288, 1323, 1345, 1424, 1491, 1529, 1913, 3113, 3183, 3752)*
$TS1_{SC1}$	1665i, 28, 52, 60, 73, 88, 126, 178, 204, 252, 287, 331, 354, 366, 414, 457, 487, 526, 544, 564, 611, 685, 755, 787, 861, 872, 949, 1036, 1123, 1196, 1220, 1260, 1266, 1306, 1318, 1405, 1431, 1478, 1911, 3162, 3761 *(1744i, 19, 46, 54, 77, 84, 120, 176, 199, 251, 286, 326, 334, 358, 420, 459, 481, 534, 551, 569, 619, 692, 766, 806, 877, 887, 965, 1051, 1149, 1197, 1242, 1279, 1284, 1306, 1340, 1351, 1430, 1465, 1505, 1948, 3222, 3882)*
$TS2_{SC1}$	913i, 19, 29, 53, 57, 70, 88, 161, 203, 249, 282, 317, 329, 410, 452, 493, 522, 541, 559, 609, 671, 752, 780, 858, 864, 930, 952, 1134, 1138, 1221, 1258, 1263, 1266, 1321, 1326, 1398, 1449, 1952, 3195 *(1166i, 29, 36, 42, 46, 70, 86, 170, 198, 248, 286, 309, 332, 416, 455, 490, 531, 550, 565, 618, 682, 765, 797, 876, 898, 963, 9836, 1147, 1163, 1243, 1270, 1286, 1289, 1346, 1347, 1433, 1472, 1981, 3245)*
$TS1_{SC2}$	1572i, 16, 40, 43, 58, 81, 103, 172, 200, 219, 251, 291, 328, 335, 417, 460, 531, 542, 563, 616, 660, 748, 774, 801, 825, 882, 964, 1071, 1128, 1173, 1238, 1278, 1279, 1308, 1330, 1341, 1450, 1474, 1490, 1972, 3228, 3888 *(1452i, 29, 45, 51, 66, 84, 93, 170, 204, 215, 249, 290, 318, 330, 411, 457, 523, 533, 557, 608, 651, 751, 775, 793, 813, 873, 947, 1048, 1116, 1179, 1219, 1257, 1261, 1299, 1310, 1317, 1417, 1451, 1498, 1935, 3169, 3765)*
$PC1_{SC1}$	23, 35, 56, 73, 89, 106, 113, 152, 163, 206, 209, 254, 280, 336, 367, 399, 421, 467, 529, 540, 566, 619, 645, 679, 765, 795, 884, 957, 1170, 1180, 1246, 1274, 1278, 1326, 1340, 1446, 1512, 1683, 1965, 3371, 3967, 4089 *(21, 36, 40, 79, 91, 104, 151, 188, 206, 211, 252, 257, 281, 309, 331, 369, 418, 458, 506, 527, 560, 612, 632, 667, 753, 769, 867, 942, 1144, 1174, 1230, 1249, 1259, 1311, 1321, 1414, 1487, 1618, 1942, 3293, 3877, 3999)*
$PC2_{SC2}$	33, 46, 64, 78, 88, 106, 154, 199, 209, 250, 261, 283, 292, 314, 330, 367, 417, 459, 499, 528, 560, 610, 618, 666, 753, 769, 868, 943, 1146, 1181, 1228, 1249, 1258, 1303, 13111416, 1489, 1622, 1939, 3292, 3875, 3995 *(55, 81, 86, 94, 117, 146, 168, 208, 219, 253, 303, 333, 344, 389, 401, 413, 459, 529, 542, 556, 607, 658, 751, 804, 848, 931, 1006, 1074, 1202, 1227, 1237, 1288, 1323, 1345, 1424, 1491, 1529, 1913, 3113, 3183, 3752)*
$CF_3C(O)OCHCF_3$	22, 33, 58, 82, 131, 199, 252, 273, 318, 337, 419, 450, 463, 532, 565, 588, 623, 677, 766, 793, 886, 959, 1171, 1214, 1250, 1271, 1323, 1343, 1443, 1519, 1965, 3348 *(24, 35, 62, 80, 129, 199, 251, 311, 331, 411, 454, 460, 524, 557, 584, 613, 665, 753, 776, 870, 942, 1143, 1196, 1223, 1250, 1261, 1302, 1317, 1407, 1485, 1933, 3283)*
H_2O	1596, 3887, 4012 *(1637, 3975, 4101)*
HCl	3031 *(3085)*

CH_3COCH_3: −52.23 kcal mol^{-1} [29], $CH_3C(O)OCH_2CH_3$: −106.46 kcal mol^{-1} [29], $CH_3C(O)OCH_3$: −98.0 kcal mol^{-1} [30] and $CF_3C(O)OCH_3$: −237.00 kcal mol^{-1} [15] to evaluate the required enthalpies of formation. The calculated values of enthalpies of formation, $\Delta_f H^\circ_{298}$ values are reported in Table 3. First the $\Delta_f H^\circ_{298}$ values for the SC1 and SC2 conformers of $CF_3C(O)OCH_2CF_3$ are obtained from the average of results obtained from the three isodesmic reactions (R3)–(R5). Then the $\Delta_f H^\circ_{298}$ value for $CF_3C(O)OCH_2CF_3$ is determined from the weighted average of the $\Delta_f H^\circ_{298}$ values for the SC1 and SC2 conformers of $CF_3C(O)OCH_2CF_3$ as described in Eq. (5). As can be seen from Table 3, the values of $\Delta_f H^\circ_{298}$ for the species obtained from the isodesmic reactions at three levels are very consistent with each other. The $\Delta_f H^\circ_{298}$ values for $CF_3C(O)OCH_2CF_3$ are −399.11, −400.66 and −400.22 kcal mol^{-1}, respectively at G2(MP2), MPWB1K/6-31+G(d,p) and M06-2X/6-31+G(d,p) levels of theory. The $\Delta_f H^\circ_{298}$ values for $CF_3C(O)OCHCF_3$ radical calculated from G2(MP2), MPWB1K/6-31+G(d,p) and M06-2X/6-31+G(d,p) results are −348.70, −350.07 and −350.08 kcal mol^{-1}, respectively. The calculated bond dissociation enthalpy (BDE) for C–H bond in $CF_3C(O)OCH_2CF_3$ is found to be 102.55 kcal mol^{-1} at G2(MP2) method. Moreover, because of the lack of the experimental values for the $\Delta_f H^\circ_{298}$ of the species involved in the title reactions, it is difficult to make a direct comparison between theoretical and experimental enthalpy of formation.

2.1. Rate constants

The rate constant for title reactions are calculated by using canonical transition state theory (CTST) [31] given by the following expression:

$$k = \sigma\Gamma(T)\frac{k_B T}{h}\frac{Q^{\ddagger}_{TS}}{Q_R}\exp\frac{-\Delta E}{RT} \quad (1)$$

Table 3
Enthalpies of formation ($\Delta_f H^\circ_{298}$) (kcal mol^{-1}) of $CF_3C(O)OCH_2CF_3$ and $CF_3C(O)OCHCF_3$ radical at G2(MP2), MPWB1K/6-31+G(d,p) and M06-2X/6-31+G(d,p) levels of theory.

Species	Isodesmic reaction	$\Delta_f H^\circ_{298}$, 298		
		G2(MP2)	MPWB1K	M06-2X
$CF_3C(O)OCH_2CF_3$ (SC1)	R3	−401.01	−399.79	−399.31
	R4	−395.11	−401.40	−400.65
	R5	−401.48	−401.02	−401.21
Average (SC1)		−399.20	−400.73	−400.39
$CF_3C(O)OCH_2CF_3$ (SC2)	R3	−400.67	−399.52	−398.66
	R4	−394.77	−401.13	−400.56
	R5	−401.14	−400.75	−400.56
Average (SC2)		−398.86	−400.46	−399.74
$CF_3C(O)OCH_2CF_3$[a]		−399.11	−400.66	−400.22
$CF_3C(O)OCHCF_3$	R6	−349.12	−353.04	−351.47
	R7	−345.61	−346.45	−347.60
	R8	−351.39	−350.72	−351.19
Average		−348.70	−350.07	−350.08

[a] Weighted average as per Boltzmann distribution law and as described in Eq. (5).

where σ is the symmetry number, $\Gamma(T)$ is the tunneling correction factor at temperature T. $Q^{\ddagger}_{TS}$ and Q_R are the total partition function (per unit volume) for the transition states and reactants, respectively. ΔE is the barrier height, k_B is the Boltzmann constant and h is the Plank's constant. R represents the universal gas constant. The value of σ is taken as 2 for this reaction channel due to the presence of two equivalent H-atoms. The electronic partition function of the OH radicals was calculated by considering the splitting of 139.7 cm^{-1} in the $^2\Pi$ ground state into account. Similarly, electronic partition function for Cl atom was evaluated by taking the splitting of 881 cm^{-1} between the ground $^2P_{3/2}$ and excited $^2P_{1/2}$ electronic states of Cl atom due to spin-orbit coupling. The partition functions for the respective transition state and reactants at 298 K are obtained from the vibrational frequencies calculation made at M06-2X/6-31+G(d,p) level. The tunneling correction $\Gamma(T)$ was estimated by using the Eckart's unsymmetric barrier method [32,33]. Partition functions were computed under rigid rotor and harmonic oscillator (HO) approximations. The hindered-rotor approximation of Truhlar and Chuang [34] was used for calculating the partition function of lower vibration modes. As discussed before, the H-abstraction by OH radicals from the $-CH_2$ group proceeds via two step mechanism. The first step involves a fast pre-equilibrium (K_{eq}) between the reactants and the hydrogen bonded reaction complex (RC) and the second step is the hydrogen abstraction with the rate constant $k_2^{\dagger}$. The overall rate constant including equilibrium constant (K_{eq}) and rate constant ($k_2^{\dagger}$) are given by,

$$K_{eq} = \frac{Q_{RC}}{Q_A \cdot Q_B} e^{(E_R - E_{RC})/RT} \quad (2)$$

and $k_2^{\dagger}$ can be obtained from TST in the from

$$k_2^{\dagger} = \sigma\Gamma(T)\frac{k_B T}{h}\frac{Q_{TS}}{Q_{RC}} e^{-(E_{TS}-E_{RC})/RT} \quad (3)$$

The rate constant for H-abstraction from $CF_3C(O)OCH_2CF_3$ via reaction (R1) is then obtained by the following expression,

$$k = K_{eq} \times k_2^{\dagger} = \sigma\Gamma(T)\frac{k_B T}{h}\frac{Q_{TS}}{Q_A \cdot Q_B} e^{-(E_{TS}-E_R)/RT} \quad (4)$$

where Q_A, Q_B, Q_{RC} and Q_{TS} represent the total partition functions (per unit volume) of the reactants, reaction complex and transition states, respectively. E_{TS}, E_{RC} and E_R are the total energies (ZPE corrected) of transition state, reaction complex and reactants, respectively. Thus, it seems that the final expression (Eq. (4)) for estimating rate constant and barrier height turns out to be the usual CTST expression (Eq. (1)) used for the determination of rate constant and barrier height of a direct reaction, irrespective of the energy of pre-reactive hydrogen bonded complex (RC). However, the tunneling factor $\Gamma(T)$ will obviously be different due to pre- and post-reaction complexes formation and as a result will affect the total rate constant. The total rate constant (k_{OH}) at temperature T is then estimated from the weighted average of the rate constant values for k_{SC1} and k_{SC2} as:

$$k(T) = W_{SC1}(T)k_{SC1}(T) + W_{SC2}k_{SC2}(T) \quad (5)$$

The W_{SC1} and W_{SC2} are the temperature dependent weight factors estimated from the Boltzmann population distribution law [35]. The W_{SC1} is calculated as $1/(1+\exp(-\Delta E/RT))$, where ΔE is the energy difference between the SC1 and SC2 conformer; and $W_{SC2} = 1 - W_{SC1}$. The rate constant for H atom abstraction reaction of $CF_3C(O)OCH_2CF_3$ by OH radicals and Cl atoms as given by reactions (R1)–(R2) are calculated to be 1.20×10^{-13} and 0.98×10^{-15} cm^3 molecule^{-1} s^{-1}, respectively at 298 K. The calculated rate constant values for H atom abstraction reaction of $CF_3C(O)OCH_2CF_3$ by OH radical are in very good agreement with the experimental values 1.05×10^{-13} cm^3 molecule^{-1} s^{-1} reported by Blanco and Teruel [21]. For the H atom abstraction reaction of $CF_3C(O)OCH_2CF_3$ by Cl atoms initiation, our calculated value (0.98×10^{-15} cm^3 molecule^{-1} s^{-1}) is in reasonable agreement with the available experimental data 1.18×10^{-15} cm^3 molecule^{-1} s^{-1} reported by Blanco et al. [20]. The rate constant calculation indicates that the M06-2X functional using 6-31+G(d,p) basis set provide a more accurate prediction of the relative energy as compared to MPWB1K method. As a result, the reaction kinetics of TFETFA with OH radicals was calculated by using M06-2X level and was found to give reliable results.

2.2. Atmospheric Implications

In general, tropospheric lifetime (τ_{eff}) of TFETFA can be estimated by assuming that its removal from troposphere occurs only through the reactions with OH radical and Cl atom. Then (τ_{eff}) can be expressed as [36],

$$\frac{1}{\tau_{eff}} = \frac{1}{\tau_{OH}} + \frac{1}{\tau_{Cl}} \quad (6)$$

where $(\tau_{OH}) = (k_{OH} \times [OH])^{-1}$ and $(\tau_{Cl}) = (k_{Cl} \times [Cl])^{-1}$. Using the 298 K value of $k_{OH} = 1.20 \times 10^{-13}$ cm^3 molecule^{-1} s^{-1} and $k_{Cl} = 0.98 \times 10^{-15}$ cm^3 molecule^{-1} s^{-1}, and the global average atmospheric OH and Cl concentrations of 2.0×10^6 and 1.0×10^4 molecule cm^{-3}, respectively [37,38], the estimated atmospheric lifetime of TFETFA is found to be 0.15 years which is in very good agreement with previous study [13].

3. Conclusions

The potential energy surface and reaction kinetics of the H atom abstraction reactions of $CF_3C(O)OCH_2CF_3$ with OH radicals and Cl atoms are investigated at M06-2X/6-31+G(d,p) level of theory. Two most stable conformers of the $CF_3C(O)OCH_2CF_3$ molecule (SC1 and SC2) are identified and their energy difference is found to be only 0.65 kcal mol^{-1}. The hydrogen abstraction reaction by OH radicals is found to follow an indirect path through the formation of pre- and post-reaction complexes. The barrier height for dominant pathways is found to be 2.17 kcal mol^{-1}. The thermal rate constant for the H atom abstraction of $CF_3C(O)OCH_2CF_3$ by OH radicals and Cl atoms are found to be 1.20×10^{-13} cm^3 molecule^{-1} s^{-1} and 0.98×10^{-15} cm^3 molecule^{-1} s^{-1} at 298 K using Canonical transition state theory which are in good agreement with experimental data. Our results

also confirm that M06-2X method coupled with 6-31+G(d,p) basis set is good for kinetic and thermochemistry for hydrogen abstraction reactions. From our theoretical study along with experimental evidence it can be concluded that hydrogen abstraction by OH radicals is both kinetically and thermodynamically more favorable than that of Cl atom initiated oxidation. The $\Delta_f H^{\circ}_{298}$ values for $CF_3C(O)OCH_2CF_3$ and $CF_3C(O)OCHCF_3$ radical calculated from G2(MP2) results are −399.11 and −348.70 kcal mol^{-1}, respectively. The estimated atmospheric lifetime of TFETFA is expected to be 0.15 years. These data can be useful for further thermo-kinetic modeling of other reactions involving these species.

4. Computational methods

Geometry optimization of the reactants, products and transition states were made at the M06-2X level of theory [39] using 6-31+G(d,p) basis set. The M06-2X/6-31+G(d,p) method was reported to be sufficiently accurate for predicting reliable geometries and frequencies of the stationary points in earlier studies [40–43]. Since the 6-31+G(d,p) basis set was used for developing the model functional, therefore it has been considered for present study. Since the formation of pre- and post-reaction complexes modifies the shape of potential energy surface for the reaction and hence affects the tunneling factor [7,12]. As a result the rate constant for hydrogen abstraction also changes. Thus we also validated pre- and post-reactive complexes along the entry and exit of the reaction path. Two reactant complexes (RCs) and product complexes (PCs) are validated at the entrances and exits of the two H-abstraction channels by OH radicals, which means that this abstraction channels may proceed via indirect mechanism. The unrestricted formalism was used for quantum chemical calculations of the open-shell TS and radicals. The $\langle S^2 \rangle$ value never found to exceed 0.761 indicating that the spin-contamination was not serious for the present system. In addition to this, to validate the accuracy of the structure and energies of the stationary points, calculations are also performed at MPWB1K/6-31+G(d,p) [44,45] level of theory using same basis set. In order to determine the nature of different stationary points on the potential energy surface, vibrational frequencies calculations were performed using the same level of theory at which the optimization was made. All the stationary points had been identified to correspond to stable minima by ascertaining that all the vibrational frequencies had real positive values. The transition states were characterized by the presence of only one imaginary frequency (NIMAG = 1). To ascertain that the identified transition states connect reactant and products smoothly, intrinsic reaction coordinate (IRC) calculations [24] were performed at the M06-2X/6-31+G(d,p) level. The M06-2X is a hybrid meta-DFT method with a high percentage of HF exchange and it is reported that the M06-2X functional gives excellent results for calculating the barrier of a reaction [46]. Single point energy calculations of the barrier heights were carried out using M06-2X with Pople's spilt-valence triple-ζ quality 6-311++G(d,p) basis set [47] and Aug-cc-pVTZ [48] basis sets with optimized geometry at M06-2X/6-31+G(d,p) level of theory. All calculations were performed with the Gaussian 09 suite of program [49]. As we mention that the two most stable conformers (SC1 and SC2) of $CF_3C(O)OCH_2CF_3$ are very close in energy. Therefore any thermodynamic quantity (Q) for $CF_3C(O)OCH_2CF_3$ at temperature T is estimated from the weighted average of that quantity for the SC1 (Q_{SC1}) and SC2 (Q_{SC2}) conformers of $CF_3C(O)OCH_2CF_3$ as:

$$Q = W_{SC1}Q_{SC1} + W_{SC2}Q_{SC2} \quad (7)$$

where W_{SC1} and W_{SC2} are the temperature dependent weight factors according to the Boltzmann distribution law [35].

Acknowledgments

The authors acknowledge financial support from the Department of Science and Technology, New Delhi in the form of a project (SR/NM.NS-1023/2011(G)). BKM is thankful to University Grants Commission, New Delhi for financial support. NKG and HJS are thankful to the Council of Scientific and Industrial Research, New Delhi for financial support. We are also thankful to the reviewers for the constructive suggestions to improve the quality of the article.

References

[1] W.T. Tsai, J. Hazard. Mater. 119 (2005) 69–78.
[2] A. Sekiya, S. Misaki, J. Fluorine Chem. 101 (2000) 215–221.
[3] R.L. Powell, J. Fluorine Chem. 114 (2002) 237–250.
[4] S. Urata, A. Takada, T. Uchimaru, A.K. Chandra, Chem. Phys. Lett. 368 (2003) 215–223.
[5] H.J. Singh, B.K. Mishra, J. Mol. Model. 17 (2011) 415–422.
[6] H.J. Singh, B.K. Mishra, J. Mol. Model. 16 (2010) 1473–1480.
[7] A.K. Chandra, J. Mol. Model. 18 (2012) 4239–4247.
[8] L. Chen, S. Kutsuna, K. Tokuhashi, A. Sekiya, Chem. Phys. Lett. 400 (2004) 563–568.
[9] H.J. Singh, B.K. Mishra, P.K. Rao, Bull. Korean Chem. Soc. 31 (2010) 3718–3722.
[10] H.J. Singh, B.K. Mishra, J. At. Mol. Sci. 4 (2013) 210–224.
[11] N. Oyaro, S.R. Sellevag, C.J. Nielsen, J. Phys. Chem. A 109 (2005) 337–346.
[12] M. Lily, D. Sutradhar, A.K. Chandra, Comput. Theor. Chem. 1022 (2013) 50–58.
[13] I. Bravo, Y. Dıaz-de-Mera, A. Aranda, E. Moreno, D.R. Nutt, G. Marston, Phys. Chem. Chem. Phys. 13 (2011) 17185–17193.
[14] A.K. Chakrabartty, B.K. Mishra, D. Bhattacharjee, R.C. Deka, Mol. Phys. 111 (2013) 860–867.
[15] B.K. Mishra, A.K. Chakrabartty, R.C. Deka, J. Mol. Model. 19 (2013) 2189–2195.
[16] M.B. Blanco, I. Bejan, I. Barnes, P. Wiesen, M.A. Teruel, Environ. Sci. Technol. 44 (7) (2010) 2354–2359.
[17] N. Oyaro, S.R. Sellevag, C.J. Neilsen, Environ. Sci. Technol. 38 (2004) 5567–5576.
[18] A. Jordan, H. Frank, Environ. Sci. Technol. 33 (4) (1999) 522–527.
[19] M.E.D. Lestard, M.E. Tuttolomondo, E.L. Varetti, D.A. Wann, H.E. Robertson, D.W.H. Rankin, A.B. Altabef, J. Mol. Struct. 917 (2009) 183–192.
[20] M.B. Blanco, I. Bejan, I. Barnes, P. Wiesen, M.A. Teruel, Chem. Phys. Lett. 453 (2008) 18–23.
[21] M.B. Blanco, M.A. Teruel, Atmos. Environ. 41 (34) (2007) 7330–7338.
[22] T.N.N. Stein, L.K. Christensen, J. Platz, J. Sehested, O.J. Nielsen, T.J. Wallington, J. Phys. Chem. A 103 (1999) 5705–5713.
[23] M.B. Blanco, I. Barnes, M.A. Teruel, J. Phys. Org. Chem. 23 (2010) 950–954.
[24] C. Gonzalez, H.B. Schlegel, J. Chem. Phys. 90 (1989) 2154–2161.
[25] J.Y. Wu, J.Y. Liu, Z.S. Li, C.C. Sun, Chem. Phys. Carbon 5 (2004) 336–1344.
[26] J. Csontos, Z. Rolik, S. Das, M. Kallay, J. Phys. Chem. A 114 (2010) 13093–13103.
[27] S.S. Chen, A.S. Rodgers, J. Chao, R.C. Wilhoit, B.J. Zwolinski, J. Phys. Chem. Ref. Data 4 (1975) 441–456.
[28] L. Wang, Y. Zhao, J. Zhang, Y. Dai, J. Zhang, Theor. Chem. Acc. 128 (2011) 183–189.
[29] K.B. Wiberg, L.S. Crocker, K.M. Morgan, J. Am. Ceram. Soc. 113 (1991) 3447–3450.
[30] H.K. Hall Jr., J.H. Baldt, J. Am. Ceram. Soc. 93 (1971) 140–145.
[31] K.J. Laidler, Chemical Kinetics, 3rd ed., Pearson Education, New Delhi, 2004.
[32] R.L. Brown, J. Res. Natl. Bur. Stand. 86 (1981) 357–359.
[33] R. Xiao, M. Noerpel, H.L. Luk, Z. Wei, R. Spinney, Int. J. Quantum Chem. 114 (2014) 74–83.
[34] Y.Y. Chuang, D.G. Truhlar, J. Chem. Phys. 112 (2000) 1221–1228.
[35] D.A. McQuarrie, Statistical Mechanics, VIVA, New Delhi, 2003.
[36] V.C. Papadimitriou, K.G. Kambanis, Y.G. Lazarou, P. Papagiannakopoulos, J. Phys. Chem. A 108 (2004) 2666–2674.
[37] R. Hein, P.J. Crutzen, M. Heimann, Global Biogeochem. Cycles 1 (1997) 43–76.
[38] O.W. Wingenter, M.K. Kubo, N.J. Blake, T.W. Smith, D.R. Blake, F.S. Rowland, J. Geophys. Res. 101 (1996) 4331–4340.
[39] Y. Zhao, D.G. Truhlar, Theor. Chem. Acc. 120 (2008) 215–241.
[40] D. Mandal, C. Sahu, S. Bagchi, A.K. Das, J. Phys. Chem. A 117 (2013) 3739–3750.
[41] T.C. Dinadayalane, G. Paytakov, J. Leszczynski, J. Mol. Model. 19 (2013) 2855–2864.
[42] A. Nijamudheen, D. Jose, A. Shine, A. Datta, J. Phys. Chem. Lett. 3 (2012) 1493–1496.
[43] L. Sandhiya, P. Kolandaivel, K. Senthilkumar, Struct. Chem. 23 (2012) 1475–1488.
[44] Y. Zhao, D.G. Truhlar, J. Phys. Chem. A 108 (2004) 6908–6918.
[45] A.K. Chakrabartty, B.K. Mishra, D. Bhattacharjee, R.C. Deka, J. Fluorine Chem. 154 (2013) 60–66.
[46] A. Beste, A.C. Buchanan, Energy Fuels 24 (2010) 2857–2867.
[47] R. Krishnan, J.S. Binkley, R. Seeger, J.A. Pople, J. Chem. Phys. 72 (1980) 650.
[48] T.H. Dunning, J. Chem. Phys. 90 (1989) 1007–1023.
[49] M.J. Frisch, G.W. Trucks, H.B. Schlegel, G.E. Scuseria, M.A. Robb, J.R. Cheeseman, G. Scalmani, V. Barone, B. Mennucci, G.A. Petersson, H. Nakatsuji, M. Caricato, X. Li, H.P. Hratchian, A.F. Izmaylov, J. Bloino, G. Zheng, J.L. Sonnenberg, M. Hada, M. Ehara, K.

Toyota, R. Fukuda, J. Hasegawa, M. Ishida, T. Nakajima, Y. Honda, O. Kitao, H. Nakai, T. Vreven, J.A. Montgomery Jr., J.E. Peralta, F. Ogliaro, M. Bearpark, J.J. Heyd, E. Brothers, K.N. Kudin, V.N. Staroverov, R. Kobayashi, J. Normand, K. Raghavachari, A. Rendell, J.C. Burant, S.S. Iyengar, J. Tomasi, M. Cossi, N. Rega, N.J. Millam, M. Klene, J.E. Knox, J.B. Cross, V. Bakken, C. Adamo, J. Jaramillo, R. Gomperts, R.E. Stratmann, O. Yazyev, A.J. Austin, R. Cammi, C. Pomelli, J.W. Ochterski, R.L. Martin, K. Morokuma, V.G. Zakrzewski, G.A. Voth, P. Salvador, J.J. Dannenberg, S. Dapprich, A.D. Daniels, Ö. Farkas, J.B. Foresman, J.V. Ortiz, J. Cioslowski, D.J. Fox, Gaussian 09, Revision B. 01, Gaussian, Inc., Wallingford, CT, 2009.